© 2025 Journal of Pharmacy & Pharmacognosy Research, 13 (3), 968-978, 2025
ISSN 0719-4250
https://jppres.com

DOI: https://doi.org/10.56499/jppres24.2153_13.3.968

Original Article

Improving the anticancer efficacy of tetrahydrocurcumin via β-cyclodextrin inclusion complexation

[Mejora de la eficacia anticancerígena de la tetrahidrocurcumina mediante la inclusión de complejos de β-ciclodextrina]

Firli Rahmah Primula Dewi[1]*, Verah Elfianah[1], Adyn Haura Mahira[1], Halimatus Sa'diah Aulia[1], Justitia Eka Putra[1], Suat Cheng Tan[2], Vuanghao Lim[3], Manikya Pramudya[1], Sri Puji Astuti Wahyuningsih[1]

[1]Department of Biology, Faculty of Science and Technology, Universitas Airlangga, Surabaya 60115, Indonesia.
[2]School of Health Sciences, Health Campus, Universiti Sains Malaysia, 16150 Kubang Kerian, Malaysia.
[3]Advanced Medical and Dental Institute, Universiti Sains Malaysia, Bertam 13200 Kepala Batas, Penang, Malaysia.
*E-mail: firli.rahmah@fst.unair.ac.id

Abstract

Context: Tetrahydrocurcumin (THC) exhibits superior biological and pharmacological characteristics compared to curcumin, demonstrating efficacy in suppressing tumor metastasis and angiogenesis and acting as a potent preventive agent against carcinogenesis. However, its limited water solubility restricts its application in aqueous formulations.

Aims: To evaluate the efficacy of a β-cyclodextrin (β-CD)-THC inclusion complex in combating colon and liver cancer in animal models. Female rats (n=24) were divided into six groups and induced with colon and liver cancer using 1,2-dimethylhydrazine (DMH).

Methods: THC or the β-CD-THC inclusion complex was orally administered twice weekly for 11 weeks. Animals were euthanized, and blood serum, colon, and liver samples were collected for analysis.

Results: Results indicate that the THC inclusion complex significantly reduced high dysplasia in the colon, decreased necrotic hepatocytes, and reduced central vein diameter in the liver. Moreover, it lowered serum levels of gamma-glutamyl transferase (GGT), matrix metalloproteinase (MMP)-2, and MMP-9 in cancer-induced rats, highlighting enhanced anticancer properties when THC is complexed with β-CD.

Conclusions: These findings underscore the potential of the β-CD-THC inclusion complex as a promising therapeutic strategy against colon and liver cancer.

Keywords: colonic neoplasms; liver neoplasms; tetrahydrocurcumin; matrix metalloproteinase.

Resumen

Contexto: La tetrahidrocurcumina (THC) exhibe características biológicas y farmacológicas superiores en comparación con la curcumina, demostrando eficacia en la supresión de la metástasis tumoral y la angiogénesis y actuando como un potente agente preventivo contra la carcinogénesis. Sin embargo, su limitada solubilidad en agua restringe su aplicación en formulaciones acuosas.

Objetivos: Evaluar la eficacia de un complejo de inclusión de β-ciclodextrina (β-CD)-THC en la lucha contra el cáncer de colon y de hígado en modelos animales. Se dividieron ratas hembras (n=24) en seis grupos y se les indujo cáncer de colon y de hígado utilizando 1,2-dimetilhidrazina (DMH).

Métodos: Se administró por vía oral THC o el complejo de inclusión β-CD-THC dos veces por semana durante 11 semanas. Los animales fueron sacrificados y se recogieron muestras de suero sanguíneo, colon e hígado para su análisis.

Resultados: Los resultados indican que el complejo de inclusión de THC redujo significativamente la displasia alta en el colon, disminuyó los hepatocitos necróticos y redujo el diámetro de la vena central en el hígado. Además, redujo los niveles séricos de gamma-glutamil transferasa (GGT), metaloproteinasa de matriz (MMP)-2 y MMP-9 en ratas con cáncer inducido, lo que resalta las propiedades anticancerígenas mejoradas cuando el THC se combina con β-CD.

Conclusiones: Estos hallazgos subrayan el potencial del complejo de inclusión β-CD-THC como una estrategia terapéutica prometedora contra el cáncer de colon y de hígado.

Palabras Clave: neoplasias colónicas; neoplasias hepáticas; tetrahidrocurcumina; metaloproteinasa de matriz.

ARTICLE INFO
Received: July 20, 2024.
Accepted: January 10, 2025.
Available Online: January 31, 2025.

AUTHOR INFO
ORCID:
0000-0002-7813-8435 (FRPD)
0009-0004-3721-9935 (HSA)
0000-0001-5081-0982 (VL)
0009-0008-4049-3256 (VE)
0009-0000-7537-4734 (JEP)
0000-0002-8591-7146 (MP)
0000-0002-3032-4132 (AHM)
0000-0001-5869-6096 (SCT)
0000-0003-1027-7110 (SPAW)

Abbreviations: THC: tetrahydrocurcumin; β-CD: β-cyclodextrin; GGT: gamma-glutamyl transferase; MMP-2: matrix metalloproteinase-2; MMP-9: matrix metalloproteinase-9; MCF-7: Michigan Cancer Foundation-7; VEGF: vascular endothelial growth factor; ddH_2O: double distilled water; FT-IR: fourier transform-infrared spectroscopy; IC: inclusion complex; ELISA: enzyme linked immunosorbent assay; HCl: hydrogen chloride; ANOVA: analysis of variance; MAM: methylazoxymethanol; CRC: colorectal cancer; MAPK: mitogen-activated protein kinases; JAK: janus kinase; STAT: signal transducers activators of transcription; NF-κB: nuclear factor-kappa B; Nrf2: nuclear factor erythroid 2–related factor 2; PI3K: phosphatidylinositol 3-kinase; AKT: protein kinase B; mTOR: mammalian target of rapamycin; DAMPs: damage-associated molecular patterns; HMGB1: high mobility group box 1; TLR4: toll-like receptor 4; HCC: hepatocellular carcinoma; RAGE: receptor for advanced glycation end-products; ECM: extracellular matrix.

INTRODUCTION

Cancer remains one of the most significant global health challenges, ranking as the second leading cause of death worldwide. In 2022 alone, nearly 20 million new cancer cases were diagnosed, and 9.7 million deaths were reported. Alarmingly, approximately one in five individuals will develop cancer during their lifetime, with mortality rates affecting one in nine men and one in 12 women (Bray et al., 2024). Despite considerable advancements in cancer therapies, the global incidence and mortality rates have plateaued over the past three decades (Ribaudo, 2023). Addressing this stagnation requires a deeper understanding of the molecular mechanisms driving cancer progression and the development of innovative therapeutic strategies. Researchers are increasingly focusing on targeted therapies to inhibit tumor growth, progression, and metastasis while minimizing adverse side effects (Umar et al., 2012). Among these approaches, natural compounds such as tetrahydrocurcumin (THC) have emerged as promising candidates for cancer treatment.

THC, a major metabolite of curcumin, exhibits enhanced biological and pharmacological properties compared to its precursor (Sandur et al., 2007). It has demonstrated significant anticancer effects, including inhibition of human breast cancer Michigan Cancer Foundation-7 (MCF-7) cells (Han et al., 2016), suppression of tumor metastasis (Yodkeeree et al., 2008), and inhibition of angiogenesis (Yoysungnoen et al., 2016). Additionally, THC has shown potential as a preventive agent against colon carcinogenesis (Kim et al., 1998). However, its clinical application is hindered by its extremely low water solubility, which limits its efficacy in water-based formulations. To address this issue, various nanoformulations have been developed to improve THC's solubility, including nanocomposites (Elbanna et al., 2023), microspheres (Senthilkumar et al., 2022), nanoemulgels (Sharma, 2023), and nanoemulsions (Tang et al., 2021). However, many of these formulations struggle to fully preserve THC's pharmacological activity, potentially compromising its toxicity profile, targeted delivery, and shelf life. Therefore, a safe and effective carrier system is crucial for improving the water solubility and bioavailability of THC for clinical applications.

β-Cyclodextrins (β-CDs), natural cyclic oligosaccharides, are widely used as drug carriers due to their ability to enhance the solubility and stability of poorly water-soluble drugs, as well as their excellent biocompatibility, biodegradability, and low immunogenicity (Gidwani and Vyas, 2015; Rita et al., 2011; Zafar et al., 2022). Structurally, β-CDs consist of seven D-glucopyranoside units linked by α-1,4-glucosidic bonds, forming a hollow truncated cone with hydrophobic cavities and hydrophilic exteriors (Hingerty et al., 1984; Lindner and Saenger, 1980). The hydrophobic cavity, measuring 4–8 Å in diameter (Saenger et al., 1998; Sandilya et al., 2020), is well-suited for encapsulating small hydrophobic molecules, improving their solubility and bioavailability.

A computational study demonstrated that β-CD inclusion complexes (ICs) of curcumin and THC enhance their efficacy as anticancer agents by inhibiting the binding of vascular endothelial growth factor (VEGF) to its receptor (Dewi et al., 2024). Furthermore, chitosan-loaded THC-ICs demonstrated cytotoxic effects on CaCo-2 cells, highlighting their potential as drug carriers for delivering THC into cancer cells (Fai et al., 2021). However, data on the in vivo anticancer activity of THC-ICs remain limited. In this study, β-CD was utilized to enhance the solubility and availability of THC by forming inclusion complexes. These complexes were evaluated for their anticancer efficacy using animal models of colon and hepatocellular carcinoma. This research aims to investigate the potential of THC and its β-CD complexes as effective drug delivery systems for improving anticancer outcomes *in vivo*.

MATERIAL AND METHODS

Chemicals

The chemicals and reagents used in this study, including 1,2-dimethylhydrazine, β-cyclodextrin, and tetrahydrocurcumin, were purchased from Sigma-Aldrich, USA. Capecitabine/binecap (Dexa Group, Indonesia), ethanol (Merck Millipore, USA), phosphate buffer saline (Oxoid, UK), hematoxylin-eosin staining kit (Abcam, UK), ELISA kit for rat MMP-9, MMP-2 and VEGF (Solarbio, China), and activity assay kit for GGT (Solarbio, China).

Synthesis of inclusion complex

The inclusion complexes were freshly prepared before each administration. The β-CD to THC ratio of 2:1 was based on a previous study (Carrier et al., 2007). To prepare the complexes, 0.85 grams of β-CD and a magnetic stir bar were added to a glass beaker with 12.5 mL of double distilled water (ddH_2O) at 60°C for one hour. Simultaneously, 0.48 grams of THC was dissolved in 12.5 mL of absolute ethanol with stirring at 60°C for one hour. The β-CD was then slowly added to the THC solution and stirred continuously for 2 hours at 60°C. The ethanol was allowed to evaporate by increasing the temperature to 70°C for 15 minutes. Subsequently, ddH_2O was added to reach a total volume of 50 mL, and the mixture was stirred for 4 hours at 25°C. The β-CD-THC inclusion complex solution was filtered using vacuum filtration, followed by drying in an oven at 50°C until white dry crystals formed.

Characterization of inclusion complex

Fourier transform-infrared spectroscopy (FT-IR) spectroscopy measurements of THC, β-cyclodextrin, and their inclusion complex were conducted using a PerkinElmer FT-IR Spectrometer (Spectrum Two) covering the 4000-400 cm^{-1} range. Each sample was enclosed in a diamond chamber, and spectra were promptly recorded. The background signal from an empty chamber was subtracted for each sample. The obtained spectra were then compared with a database to identify the functional groups present in each sample (Dewi et al., 2022).

Experimental design and animal treatment

All procedures involving animal models were approved by the Animal Care and Use Committee of the Faculty of Dentistry, Universitas Airlangga (Approval No. 461/HRECC.FODM/VII/2022). Twenty-four female Wistar rats (*Rattus norvegicus*), aged 6–8 weeks and weighing 250–300 g, were housed in plastic cages with wire gauze covers, with four rats per cage. The rats were maintained in a controlled environment at 24 ± 2°C, with a relative humidity of 60–70% and a 12-hour light-dark cycle (07:00–19:00). They were provided free access to food and water, with food replenished daily, and their body weight was monitored weekly throughout the study. Prior to treatment initiation, a two-week acclimatization period was observed, followed by grouping into six categories:

Normal control group (NC): injected with buffer saline.

Negative control group: injected with DMH in buffer saline.

Positive control group: injected with DMH and treated with capecitabine at a dose of 12.5 mg/kg BW.

β-CD group (BCD): injected with DMH and β-cyclodextrin.

THC group: injected with DMH, treated with THC at a dose of 75 mg/kg BW.

Inclusion complex (IC) group: injected with DMH, treated with inclusion complex equivalent in dose to the THC group.

Colon cancer was induced via intraperitoneal (i.p.) injection of DMH at a dose of 40 mg/kg BW, as per previous studies (Venkatachalam et al., 2020). DMH was administered weekly for 10 weeks. Subsequently, treatments with THC or its inclusion complex (75 mg/kg) were given orally twice weekly for 11 weeks. This dose was selected as it is lower than the THC dose used in previous studies (Yoysungneon et al., 2008; Zeng et al., 2023) and was optimized by encapsulating the same dose of THC within an inclusion complex. Animals were euthanized using ketamine injection, followed by dissection to collect blood serum, colon, and liver samples.

Body weight gain measurement

To assess cancer aggressiveness, changes in body weight were measured (Kocarnik et al., 2017). The body weight of rats was recorded before DMH treatment and again before surgery. Body weight gain was calculated by subtracting the initial body weight (g) before treatment from the body weight before surgery.

Histopathology analysis of liver and colon by hematoxylin-eosin staining

Briefly, 4-µm thick paraffin-embedded tissue blocks were sectioned onto slides and deparaffinized overnight in an oven. The slides were then stained with hematoxylin solution for 10 minutes, followed by rinsing with running water and a 5-second incubation in acidic ethanol (1% HCl in 70% ethanol). Subsequently, eosin staining was applied for 5 minutes, followed by a dehydration process using an alcohol series (70% ethanol to absolute ethanol) and xylene (xylene I and xylene II). Finally, the slides were mounted with Entellan mounting medium and observed under a Nikon microscope. Measurements of central vein diameter, counts of normal, swelling, necrotic hepatocytes, and analysis of crypt pathology were conducted using ImageJ software (Dewi et al., 2022; Schneider et al., 2012).

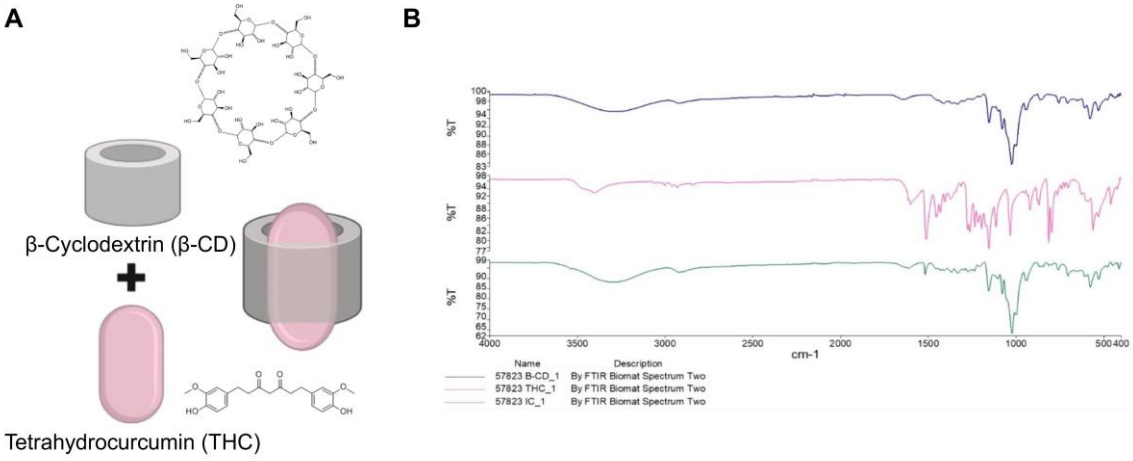

Figure 1. Characterization of the inclusion complex.
(A) The schematic illustration of the inclusion complex structure; **(B)** FT-IR analysis of THC, beta-cyclodextrin, and the inclusion complex.

Measurement of angiogenesis and invasion marker by enzyme-linked immunosorbent assay (ELISA)

Cancer invasion and angiogenesis were analyzed from blood serum samples using ELISA assays specific to MMP-2 (Solarbio, SEKR-0066), MMP-9 (Solarbio, SEKR-0027), and VEGF (Solarbio, SEKR-0032). Standard solutions (pure MMP-2, MMP-9, and VEGF proteins), wash buffers, biotin-conjugated antibody solutions, and streptavidin-HRP solutions were prepared according to kit instructions. Initially, 50 µL of standards (0, 250, 500, 1000, 2500, 5000 pg/mL) were added to each well and gently shaken. PBS (pH 7.0–7.2) was added to the blank control, while 5 µL of balance solution was added to 50 µL of each sample. After adding 50 µL of conjugate to each well (except the control), the plate was covered and incubated at 37°C for 60 minutes. Following washing and air-drying, substrate solutions A and B were added to each well, including the control, and incubated at 37°C for 15–20 minutes. The reaction was stopped with 50 µL of stop solution, mixed, and absorbance was measured at 450 nm. Absorbance values were plotted on a standard curve to determine the concentration of each biomarker. (Dewi et al., 2022; Yuan et al., 2022).

Statistical analysis

The results are presented as the mean ± standard deviation. Statistical analysis was performed using one-way analysis of variance (ANOVA) in GraphPad PRISM to determine significant differences, with a probability value of $p<0.05$ considered statistically significant. Each experiment was conducted in triplicate ($n = 3$).

RESULTS

Characteristics of the inclusion complex

To characterize the β-CD-THC inclusion complex, spectrophotometry and FT-IR analysis were employed. Spectrophotometric analysis showed that the THC solution, initially cloudy, became clear upon mixing with β-CD. To identify the interaction between THC and beta-cyclodextrin, we compared the FT-IR spectra of THC and beta-cyclodextrin with that of the inclusion complex (Fig. 1B). The spectrum of β-CD showed an absorption peak at 3300-3400 cm^{-1}, indicating O-H group stretching. Another peak at 2924 cm^{-1} is associated with C-H stretching (Rachmawati et al., 2013). Additional peaks were observed at 1152 cm^{-1} and 1022 cm^{-1}, corresponding to the stretching of C-O-C and C groups, respectively (Shahzaib, 2023). The FT-IR spectrum of THC displayed an absorption peak at 3426 cm^{-1} for the O-H group and a stretching spectrum at 3005 cm^{-1} for the C-H group. An absorption peak at 1602 cm^{-1} indicated the presence of the C-O group, while aromatic ring stretching was observed at 1515 cm^{-1}. The absorption peak at 1276 cm^{-1} signified the presence of a C-O group belonging to the enol group, and the peak at 1033 cm^{-1} indicated a stretch for the C-O-CH3 group. The absorption bands at 1458 and 1371 cm^{-1} indicated the presence of C-H groups belonging to the methyl group, and the peak at 1116 cm^{-1} indicated the presence of a C-OH group (Trivedi et al., 2020). When β-CD was combined with THC, the resulting spectrum showed absorption peaks closely resembling those of β-CD, with a peak at 1500 cm^{-1} indicating the presence of C-O groups. Based on the FT-IR spectrum of

the β-CD-THC inclusion complex, it is evident that the THC spectrum is bound to β-CD and that the synthesis process does not alter the basic structure of β-CD.

THC-inclusion complex increased body weight in rats-induced colon cancer

To determine the effect of colon cancer induction and THC-inclusion complex treatment on rat growth rates, body weight was measured before and after treatment to calculate weight gain in each group. The results showed (Fig. 2) that colon cancer induction reduced weight gain, while both THC and the inclusion complex treatment significantly increased body weight compared to the normal and negative control groups ($p<0.0001$).

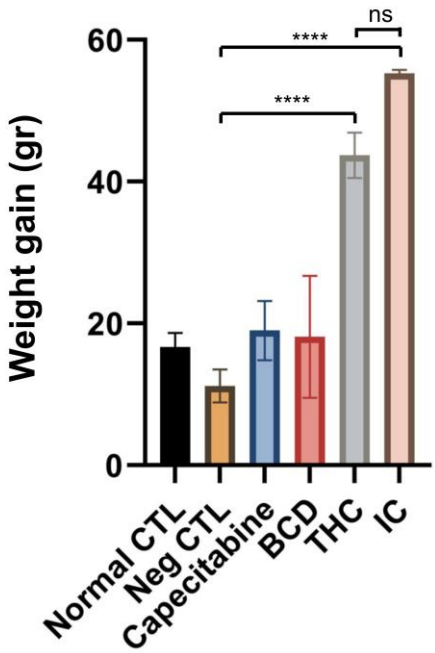

Figure 2. The body weight gain of rat's animal model following treatment with THC and inclusion complex at the dose of 75 mg/kg body weight for 11 weeks.

Data represent mean ± SD (n = 3). ****p<0.0001 significantly different, ns: not significant. CTL: control; Neg: negative; BCD: β-cyclodextrin; THC: tetrahydrocurcumin; IC: inclusion complex.

THC-inclusion complex improved the histopathology condition of the colon in rats-induced colon cancer

To assess the therapeutic potency of the THC-inclusion complex on colon cancer, a histopathological analysis of the colon was conducted. The condition of the colonic crypts was examined, and the percentages of normal crypts, lymphocyte infiltration, low-grade dysplasia, and high-grade dysplasia were determined. The results showed a significant increase in the percentage of normal crypts and a substantial reduction in high-grade dysplasia in the inclusion complex group compared to the negative control group (Fig. 3). Additionally, the histopathological condition of the colon in the inclusion complex group showed greater improvement compared to the THC group.

THC-inclusion complex reduced the diameter of the central vein in the liver and the level of GGT in the serum of rats-induced colon cancer

Methylazoxymethanol (MAM), a reactive metabolite of DMH, can alkylate macromolecules in the liver and colon (Hamiza et al., 2014). While DMH is a known procarcinogen for the liver, it also induces liver damage, such as apoptosis, and increases oxidative stress in both the liver and colon (Ramos Caetano et al., 2020). To assess hepatic damage caused by DMH and evaluate the therapeutic efficacy of the THC-inclusion complex, the diameter of the central vein in the liver and serum GGT levels were examined. The results showed a significant increase in central vein diameter in the negative control group compared to the normal control group following DMH treatment (Fig. 4). Treatment with THC alone or the inclusion complex did not significantly reduce central vein diameter; however, the inclusion complex group showed a significantly smaller diameter compared to the THC group ($p<0.05$). Additionally, serum GGT levels were significantly reduced in both the THC ($p<0.001$) and inclusion complex groups ($p<0.0001$) compared to the negative control group.

THC-inclusion complex improved the histopathology condition of the liver in rats-induced colon cancer

To further evaluate the anticancer potency of the THC-inclusion complex, the histopathological condition of the liver was analyzed in rats with DMH-induced colon cancer. The percentages of normal hepatocytes, cell swelling, and necrosis were quantified. The results revealed a significant increase in the percentage of normal hepatocytes in both the THC ($p<0.001$) and inclusion complex groups ($p<0.0001$), with the inclusion complex group showing a notably higher percentage than the THC group ($p<0.01$). Both THC ($p<0.001$) and the inclusion complex ($p<0.0001$) significantly reduced cell swelling compared to the negative control group (Fig. 5) . Additionally, the percentage of necrotic cells significantly decreased in the inclusion complex group ($p<0.0001$), but not in the THC group, compared to the negative control group. The inclusion complex group also exhibited a significantly lower percentage of necrotic cells compared to the THC group ($p<0.001$). These findings suggest that the THC-inclusion complex demonstrates superior anticancer efficacy compared to THC alone.

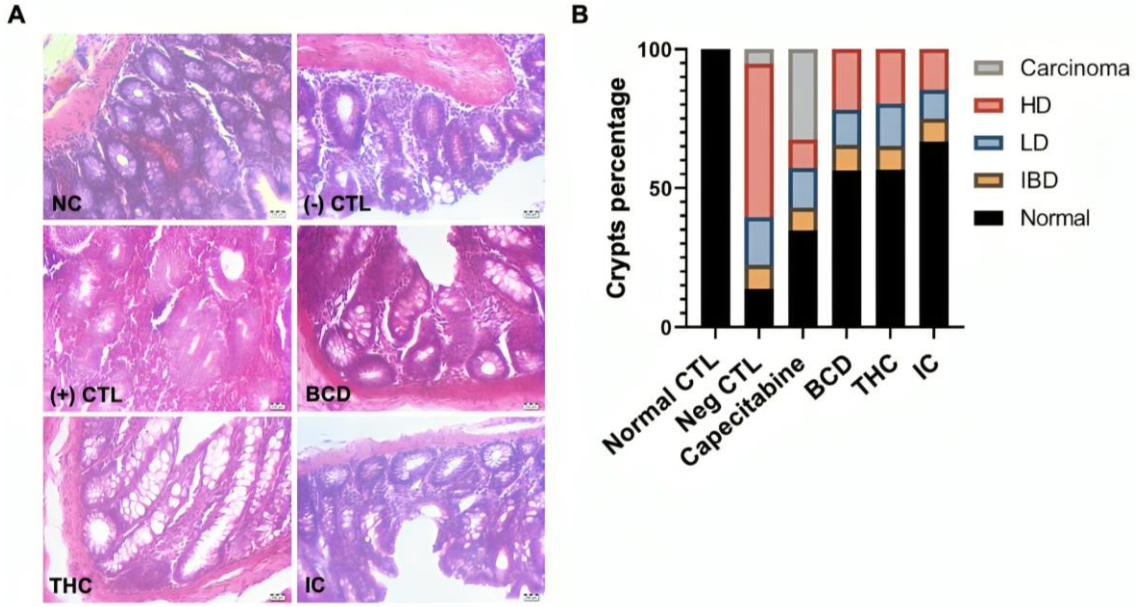

Figure 3. The colon histopathology of rat's animal model following treatment with THC and inclusion complex at the dose of 75 mg/kg body weight for 11 weeks.

(A) The representative figure of colon histology; *(B)* The percentage of normal, low-grade dysplasia, high-grade dysplasia, and carcinoma in the colon. CTL: control; Neg: negative; BCD: β-cyclodextrin; THC: tetrahydrocurcumin; IC: inclusion complex.

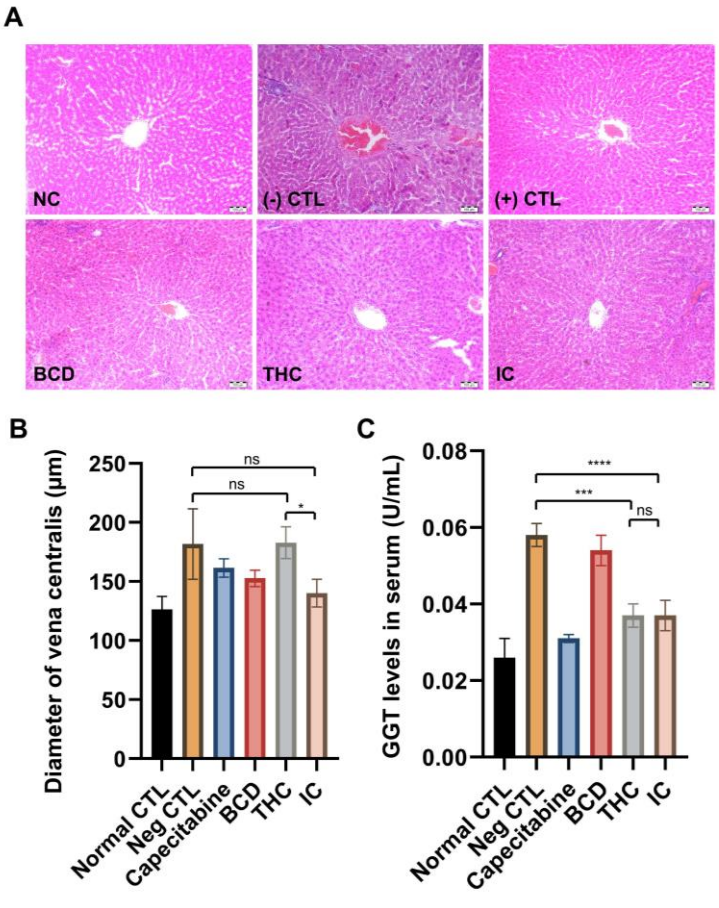

Figure 4. The liver histopathology of rat's animal model following treatment with THC and inclusion complex at the dose of 75 mg/kg body weight for 11 weeks.

(A) The representative figure of central veins; **(B)** The diameter of central veins in the liver; **(C)** The serum level of GGT. Data represent mean ± SD (n = 3). **p<0.01, ***p<0.001, ****p<0.0001 significantly different, ns: not significant. CTL: control; Neg: negative; BCD: β-cyclodextrin; THC: tetrahydrocurcumin; IC: inclusion complex.

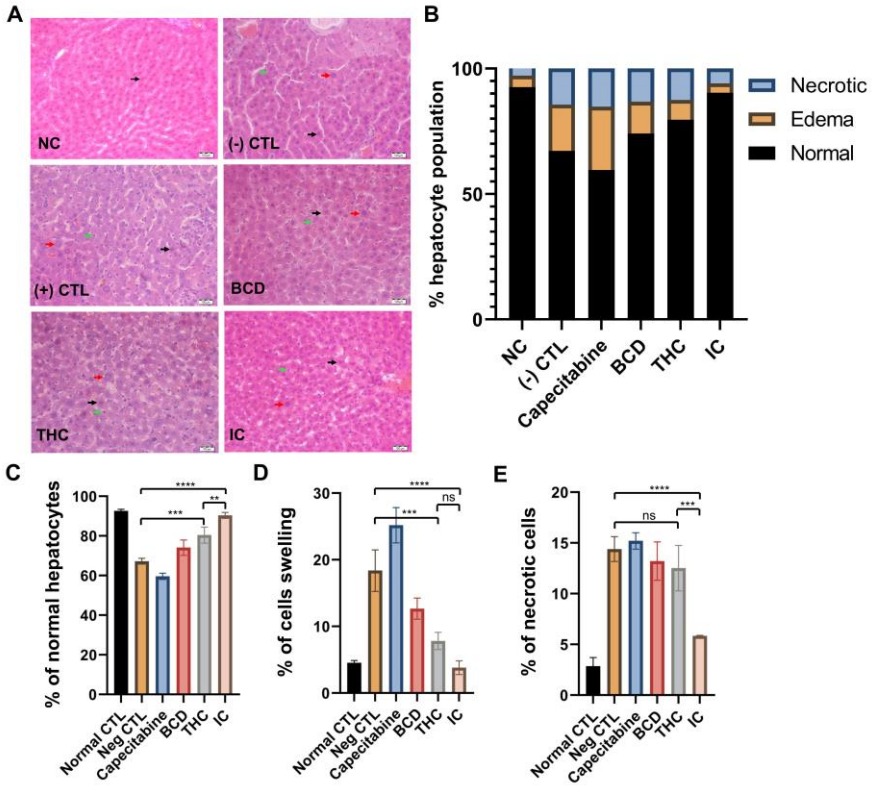

Figure 5. The percentage of normal, swelling, and necrotic hepatocytes of rat's animal model following treatment with THC and inclusion complex at the dose of 75 mg/kg body weight for 11 weeks.

(A) The representative figure of normal, swelling, and necrotic hepatocytes; **(B-E)** The percentage of normal, swelling, and necrotic hepatocytes. Data represent mean ± SD (n = 3). **p<0.01, ***p<0.001, ****p<0.0001 significantly different, ns: not significant. CTL: control; Neg: negative; BCD: β-cyclodextrin; THC: tetrahydrocurcumin; IC: inclusion complex.

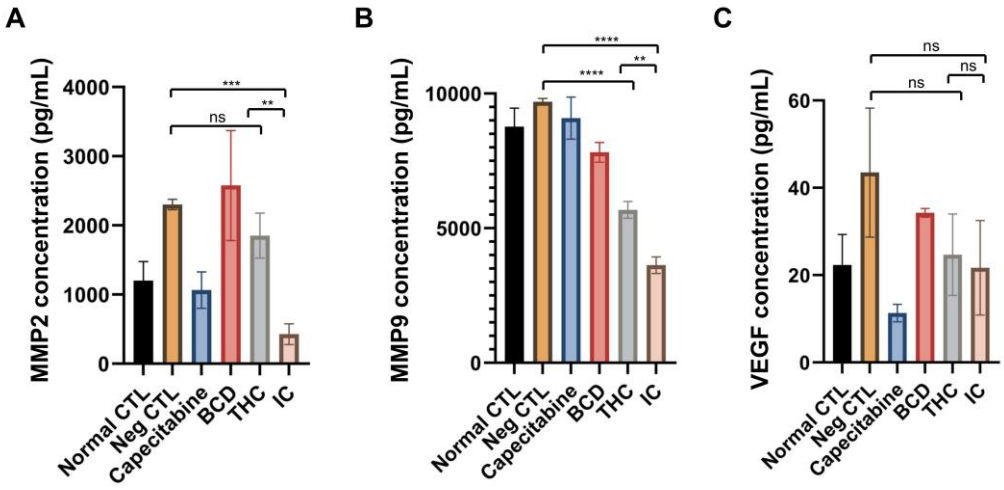

Figure 6. The serum level of angiogenesis and metastasis marker of rat's animal model following treatment with THC and inclusion complex at the dose of 75 mg/kg body weight for 11 weeks.

(A) Serum level of MMP-2; **(B)** Serum level of MMP-9; **(C)** Serum level of VEGF. Data represent mean ± SD (n = 3). **p<0.01, ***p<0.001, ****p<0.0001 significantly different, ns: not significant. CTL: control; Neg: negative; BCD: β-cyclodextrin; THC: tetrahydrocurcumin; IC: inclusion complex.

THC-inclusion complex reduced the invasion marker in rats-induced colon cancer

The anti-invasion activity of the THC-inclusion complex, the expression of angiogenesis and metastasis markers, including MMP-2, MMP-9, and VEGF, were analyzed in serum. The results revealed a significant reduction in MMP-2 levels in the inclusion complex group but not in the THC group (Fig. 6), com-

pared to the negative control group ($p<0.001$). For MMP-9, levels were significantly lower in both the THC and inclusion complex groups compared to the negative control group ($p<0.0001$). Furthermore, the inclusion complex group showed significantly reduced MMP-2 and MMP-9 expression compared to the THC group ($p<0.01$). Although VEGF levels did not differ significantly among the groups, a trend toward lower expression was observed in both the THC and inclusion complex groups. These findings underscore the enhanced anti-invasion efficacy of the THC inclusion complex.

DISCUSSION

Colorectal cancer (CRC) remains a leading global cause of mortality, with nearly 2 million new cases and 1 million deaths reported in 2020. It ranks third in cancer incidence and second in mortality (Morgan et al., 2023). CRC originates from genetic or epigenetic alterations in epithelial cells, driving uncontrolled proliferation (Testa et al., 2018). This leads to the adenoma-carcinoma sequence, a progression from normal epithelial cells to hyperplastic polyps, sessile serrated adenomas, and eventually malignancy, with inflammation playing a pivotal role in this process (Keum and Giovannucci, 2019).

In this study, DMH-induced colon cancer in rats was associated with increased occurrences of both low-grade and high-grade dysplasia. Treatment with THC and its β-CD inclusion complex effectively reduced dysplasia grades and significantly restored normal crypt architecture. THC's extensive pharmacological effects have been well-documented, particularly its ability to modulate key signaling pathways such as MAPK, JAK/STAT, NF-κB, Nrf2, and PI3K/AKT/mTOR (Lin et al., 2022; Song et al., 2018; Zeng et al., 2023). These pathways play pivotal roles in regulating inflammation, cell death, and carcinogenesis, highlighting THC's therapeutic potential in cancer treatment. Furthermore, recent studies demonstrate that the THC inclusion complex significantly reduces tumor volume in rat xenograft models (Low et al., 2024).

DMH administration is also known to induce hepatocellular damage, promoting liver carcinogenesis. Apoptosis and necrosis are the primary modes of cell death in this context, with apoptosis acting as a protective mechanism against malignant transformation, while necrosis often triggers inflammatory responses that exacerbate liver damage (Garcia-Pras et al., 2021; Gautheron et al., 2020). In this study, the inclusion complex significantly increased the proportion of normal hepatocytes and reduced necrotic cell counts compared to the native THC-treated and control groups, demonstrating its superior efficacy in maintaining liver homeostasis.

Necrosis releases damage-associated molecular patterns (DAMPs) such as high mobility group box 1 (HMGB1), which act as proinflammatory mediators, exacerbating inflammation and potentially promoting carcinogenesis (Tonnus et al., 2019). HMGB1 amplifies inflammatory responses through TLR4 activation and cytokine release, including IL-8, and has been linked to poor prognosis in hepatocellular carcinoma (Chen et al., 2015; Hernandez et al., 2019; Yu et al., 2006). By reducing necrotic cell counts, the β-CD-THC complex may limit HMGB1 release, thereby mitigating inflammatory and tumor-promoting processes in the liver.

The study also demonstrated that treatment with the inclusion complex significantly decreased serum levels of MMP-2 and MMP-9 compared to the native THC-treated and control groups. MMPs are key mediators of extracellular matrix (ECM) degradation, facilitating cancer cell invasion, migration, and angiogenesis (Lachowski et al., 2019; Weis and Cheresh, 2011). MMP-9, in particular, has been associated with colorectal malignancies and poor clinical outcomes, including larger tumors, metastasis, and higher disease stages (Jiang and Li, 2021). The observed reduction in MMP-2 and MMP-9 levels suggests that the inclusion complex effectively inhibits ECM remodeling, thereby mitigating tumor progression in both the colon and liver.

Cyclodextrin-based drug delivery systems offer a promising approach for enhancing the solubility and bioavailability of poorly soluble drugs, such as THC, while minimizing systemic toxicity. By encapsulating THC within β-CD, the inclusion complex not only improved solubility but also enhanced targeted delivery to cancer sites, reducing adverse effects and potentially overcoming drug resistance (Carrier et al., 2007; Gidwani and Vyas, 2015). Furthermore, host-guest inclusion complexes can be customized to target specific cancer cells, thereby enhancing treatment efficacy and reducing the risk of drug resistance. These complexes have also shown potential in enhancing the delivery of poorly soluble drugs, which are often challenging to administer. By encapsulating such drugs within a host molecule, their solubility and bioavailability can be significantly improved, ultimately leading to better patient outcomes (Inam, 2023). Previous research has highlighted the potential of THC inclusion complexes with CD derivatives for developing new aqueous biofungicides (Loron, 2021). This study is the first to demonstrate that the β-CD-THC inclusion complex significantly enhances the anticancer efficacy of THC in rats-induced colon and hepatocellular carcinoma, providing a foundation for

future research on its clinical application in cancer therapy.

CONCLUSION

This study highlights the potential of the β-CD-THC inclusion complex as a promising strategy to enhance the solubility and bioavailability of THC. This is evidenced by the significant improvements observed in the β-CD-THC group compared to the native THC group, including reduced high-grade dysplasia crypts, smaller vena centralis diameters, a higher percentage of normal hepatocytes, and a lower percentage of necrotic hepatocytes. Additionally, the β-CD-THC complex significantly reduced serum levels of MMP-2 and MMP-9, further supporting its enhanced anticancer efficacy. Our findings also demonstrate the complex's notable impact on ameliorating histopathological conditions in colon and liver tissues affected by cancer, with reductions in high-grade dysplasia in the colon and necrotic cell damage in the liver. The observed decrease in serum MMP-2 and MMP-9 levels suggests a critical role for the β-CD-THC inclusion complex in inhibiting angiogenesis and metastasis, underscoring its therapeutic potential in cancer treatment.

CONFLICT OF INTEREST

The authors declare no conflicts of interest.

ACKNOWLEDGMENTS

This work was funded by International Research Collaboration Top #300, Universitas Airlangga, Indonesia (grant number: 418/UN3.LPPM/PT.01.03/2024).

REFERENCES

Bray F, Laversanne M, Sung H, Ferlay J, Siegel RL, Soerjomataram I, Jemal A (2024) Global cancer statistics 2022: GLOBOCAN estimates of incidence and mortality worldwide for 36 cancers in 185 countries. CA Cancer J Clin 74(3): 229–263. https://doi.org/10.3322/caac.21834

Carrier RL, Miller LA, Ahmed I (2007) The utility of cyclodextrins for enhancing oral bioavailability. J Control Release 123(2): 78-99. https://doi.org/10.1016/j.jconrel.2007.07.018

Chen M, Liu Y, Varley P, Chang Y, He XX, Huang H, Tang D, Lotze MT, Lin J, Tsung A (2015) High-mobility group box 1 promotes hepatocellular carcinoma progression through mir-21-mediated matrix metalloproteinase activity. Cancer Res 75(8): 1645–1656. https://doi.org/10.1158/0008-5472.CAN-14-2147

Dewi FRP, Shoukat N, Alifiyah NI, Wahyuningsih SPA, Rosyidah A, Prenggono MD, Hartono H (2022) Increasing the effect of annonacin using nanodiamonds to inhibit breast cancer cells growth in rats (*Rattus norvegicus*)-Induced breast cancer. Heliyon 8(11): e11418. https://doi.org/10.1016/j.heliyon.2022.e11418

Dewi FRP, Tambunan UVD, Bari PA, Farid MA, Anjani NA, Wahyningsih SPA, Saik AYH, Keong YY, Lim V, Tan WN, Alshawsh (2024) Formation of inclusion complex of curcumin and tetrahydrocurcumin prevents angiogenesis by inhibiting VEGF activity: An *in-silico* study. Sains Malaysiana 53(3): 653–665. http://doi.org/10.17576/jsm-2024-5303-13

Elbanna SA, Ebada HMK, Abdallah OY, Essawy MM, Abdelhamid HM, Barakat HS (2023) Novel tetrahydrocurcumin integrated mucoadhesive nanocomposite κ-carrageenan/xanthan gum sponges: A strategy for effective local treatment of oral cancerous and precancerous lesions. Drug Deliv 30(1): 2254530. https://doi.org/10.1080/10717544.2023.2254530

Fai TK, Yee GH, Kumar PV, Elumalai M (2021) Preparation of chitosan particles as a delivery system for tetrahydrocurcumin: β-cyclodextrin inclusive compound for colorectal carcinoma. Curr Drug Ther 16(5): 430–438. https://doi.org/10.2174/1574885516666211210153741

Garcia-Pras E, Fernandez-Iglesias A, Gracia-Sancho J, Perez-Del-Pulgar S (2021) Cell death in hepatocellular carcinoma: Pathogenesis and therapeutic opportunities. Cancers (Basel) 14(1): 48. https://doi.org/10.3390/cancers14010048

Gautheron J, Gores GJ, Rodrigues CMP (2020) Lytic cell death in metabolic liver disease. J Hepatol 73(2): 394-408. https://doi.org/10.1016/j.jhep.2020.04.001

Gidwani B, Vyas A (2015) A comprehensive review on cyclodextrin-based carriers for delivery of chemotherapeutic cytotoxic anticancer drugs. Biomed Res Int 2015: 198268. https://doi.org/10.1155/2015/198268

Hamiza OO, Rehman MU, Khan R, Tahir M, Khan AQ, Lateef A, Sultana S (2014) Chemopreventive effects of aloin against 1,2-dimethylhydrazine-induced preneoplastic lesions in the colon of Wistar rats. Hum Exp Toxicol 33(2): 148–163. https://doi.org/10.1177/0960327113493307

Han X, Deng S, Wang N, Liu Y, Yang X (2016) Inhibitory effects and molecular mechanisms of tetrahydrocurcumin against human breast cancer MCF-7 cells. Food Nutr Res 60: 30616. https://doi.org/10.3402/fnr.v60.30616

Hernandez C, Huebener P, Pradere JP, Antoine DJ, Friedman RA, Schwabe RF (2019) HMGB1 links chronic liver injury to progenitor responses and hepatocarcinogenesis. J Clin Invest 129(4): 1803. https://doi.org/10.1172/JCI128262

Hingerty B, Klar B, Hardgrove GL, Betzel C, Saenger W (1984) Neutron diffraction of alpha, beta and gamma cyclodextrins: Hydrogen bonding patterns. J Biomol Struct Dyn 2(1): 249–260. https://doi.org/10.1080/07391102.1984.10507561

Inam M, Sareh Sadat MF, Chen W (2023) Cyclodextrin based host-guest inclusion complex, an approach to enhancing the physicochemical and biopharmaceutical application of poorly water-soluble drugs. Chem Res Chin Univ 39: 857–861. https://doi.org/10.1007/s40242-023-3204-0

Jiang H, Li H (2021) Prognostic values of tumoral MMP2 and MMP9 overexpression in breast cancer: A systematic review and meta-analysis. BMC Cancer 21(1): 149. https://doi.org/10.1186/s12885-021-07860-2

Keum N, Giovannucci E (2019) Global burden of colorectal cancer: Emerging trends, risk factors and prevention strategies. Nat Rev Gastroenterol Hepatol 16(12): 713-732. https://doi.org/10.1038/s41575-019-0189-8

Kim JM, Araki S, Kim DJ, Park CB, Takasuka N, Baba-Toriyama H, Ota T, Nir Z, Khachik F, Shimidzu N, Tanaka Y, Osawa T, Uraji T, Murakoshi M, Nishino H, Tsuda H (1998) Chemopreventive effects of carotenoids and curcumins on mouse colon carcinogenesis after 1,2-dimethylhydrazine initiation. Carcinogenesis 19(1): 81–85. https://doi.org/10.1093/carcin/19.1.81

Kocarnik JM, Hua X, Hardikar S, Robinson J, Lindor NM, Win AK, Hopper JL, Figueiredo JC, Potter JD, Campbell PT, Gallinger S, Cotterchio M, Adams SV, Cohen SA, Phipps AI, Newcomb PA (2017) Long-term weight loss after colorectal cancer diagnosis

is associated with lower survival: The Colon Cancer Family Registry. Cancer 123(23): 4701–4708. https://doi.org/10.1002/cncr.30932

Lachowski D, Cortes E, Rice A, Pinato D, Rombouts K, Del Rio Hernandez A (2019) Matrix stiffness modulates the activity of MMP-9 and TIMP-1 in hepatic stellate cells to perpetuate fibrosis. Sci Rep 9(1): 7299. https://doi.org/10.1038/s41598-019-43759-6

Lin HW, Chen TC, Yeh JH, Tsou SC, Wang I, Shen TJ, Chuang CJ, Chang YY (2022) Suppressive effect of tetrahydrocurcumin on pseudomonas aeruginosa lipopolysaccharide-induced inflammation by suppressing JAK/STAT and Nrf2/HO-1 pathways in microglial cells. Oxid Med Cell Longev 2022: 4978556. https://doi.org/10.1155/2022/4978556

Lindner K, Saenger W (1980) Crystal structure of the gamma-cyclodextrin n-propanol inclusion complex; correlation of alpha-, beta-, gamma-cyclodextrin geometries. Biochem Biophys Res Commun 92(3): 933–938. https://doi.org/10.1016/0006-291x(80)90792-5

Loron A, Gardrat C, Tabary N, Martel B, Coma V (2021) Tetrahydrocurcumin encapsulation in cyclodextrins for water solubility improvement: Synthesis, characterization and antifungal activity as a new biofungicide. Carbohydr Polym Technol Appl 2: 100113. https://doi.org/10.1016/j.carpta.2021.100113

Low ZX, Teo MYM, Nordin FJ, Palanirajan VK, Morak-Mlodawska B, Qazi AS, In LLA (2024) Enhancing the solubility and potency of tetrahydrocurcumin as an anti-cancer agent using a β-cyclodextrin inclusion complex approach. PLoS One 19(7): e0305171. https://doi.org/10.1371/journal.pone.0305171

Morgan E, Arnold M, Gini A, Lorenzoni V, Cabasag CJ, Laversanne M, Vignat J, Ferlay J, Murphy N, Bray F (2023) Global burden of colorectal cancer in 2020 and 2040: incidence and mortality estimates from GLOBOCAN. Gut 72(2): 338-344. https://doi.org/10.1136/gutjnl-2022-327736

Rachmawati H, Edityaningrum CA, Mauludin R (2013) Molecular inclusion complex of curcumin-beta-cyclodextrin nanoparticle to enhance curcumin skin permeability from hydrophilic matrix gel. AAPS PharmSciTech 14(4): 1303-1312. https://doi.org/10.1208/s12249-013-0023-5

Ramos Caetano BF, Baptista Tablas M, Ribeiro Romualdo G, Marchesan Rodrigues MA, Barbisan LF (2020) Early molecular events associated with liver and colon sub-acute responses to 1,2-dimethylhydrazine: Potential implications on preneoplastic and neoplastic lesion development. Toxicol Lett 329: 67-79. https://doi.org/10.1016/j.toxlet.2020.04.009

Ribaudo G (2023) Natural products chemistry: Advances in synthetic, analytical and bioactivity studies. Molecules 28(14): 5577. https://doi.org/10.3390/molecules28145577

Rita L, Amit T, Chandrashekhar G, Kundnani PKM (2011) Current trends in β-cyclodextrin based drug delivery systems. Int J Res Ayurveda Pharm 2(5): 1520–1526.

Saenger W, Jacob J, Gessler K, Steiner T, Hoffmann D, Sanbe H, Koizumi K, Smith SM, Takaha T (1998) Structures of the common cyclodextrins and their larger analogues-beyond the doughnut. Chem Rev 98(5): 1787-1802. https://doi.org/10.1021/cr9700181

Sandilya AA, Natarajan U, Priya MH (2020) Molecular view into the cyclodextrin cavity: structure and hydration. ACS Omega 5(40): 25655-25667. https://doi.org/10.1021/acsomega.0c02760

Sandur SK, Pandey MK, Sung B, Ahn KS, Murakami A, Sethi G, Limtrakul P, Badmaev V, Aggarwal BB (2007) Curcumin, demethoxycurcumin, bisdemethoxycurcumin, tetrahydrocurcumin and turmerones differentially regulate anti-inflammatory and anti-proliferative responses through a ROS-independent mechanism. Carcinogenesis 28(8): 1765-1773. https://doi.org/10.1093/carcin/bgm123

Schneider CA, Rasband WS, Eliceiri KW (2012) NIH Image to ImageJ: 25 years of image analysis. Nat Methods 9(7): 671–675. https://doi.org/10.1038/nmeth.2089

Senthilkumar C, Kannan PR, Balashanmugam P, Raghunandhakumar S, Santhiamurthi P, Sivakumar S, Arockiajaran A, Mary SA, Madhan B (2022) Collagen - *Annona* polysaccharide scaffolds with tetrahydrocurcumin loaded microspheres for antimicrobial wound dressing. Carbohydr Polym Technol Appl 3: 100204. https://doi.org/10.1016/j.carpta.2022.100204

Shahzaib A, Shaily, Ahmad I, Zafar F, Alshehri SM, Ali S, Nishat N (2023) One pot synthesis of cyclodextrin MOF as a promising heterogeneous catalyst for the reduction of nitroaromatic compounds and azo dyes. Res Chem Intermed 49(6): 2507–2528. https://doi.org/10.1007/s11164-023-04986-9

Sharma K (2023) Nanoemulgel formulation of tetrahydrocurcumin with efficient anti-inflammatory effect for the treatment of skin disorders. Ind J Pharm Edu Res 57(3s): s528-s539. https://doi.org/10.5530/ijper.57.3s.61

Song G, Lu H, Chen F, Wang Y, Fan W, Shao W, Lu H, Lin B (2018) Tetrahydrocurcumin-induced autophagy via suppression of PI3K/Akt/mTOR in non-small cell lung carcinoma cells. Mol Med Rep 17(4): 5964–5969. https://doi.org/10.3892/mmr.2018.8600

Tang X, Dong Q, Li J, Li F, Michniak-Kohn BB, Zhao D, Ho CT, Huang Q (2021) Anti-melanogenic mechanism of tetrahydrocurcumin and enhancing its topical delivery efficacy using a lecithin-based nanoemulsion. Pharmaceutics 13(8): 1185. https://doi.org/10.3390/pharmaceutics13081185

Testa U, Pelosi E, Castelli G (2018) Colorectal cancer: genetic abnormalities, tumor progression, tumor heterogeneity, clonal evolution and tumor-initiating cells. Med Sci (Basel) 6(2): 31 https://doi.org/10.3390/medsci6020031

Tonnus W, Meyer C, Paliege A, Belavgeni A, von Massenhausen A, Bornstein SR, Hugo C, Becker JU, Linkermann A (2019) The pathological features of regulated necrosis. J Pathol 247(5): 697–707. https://doi.org/10.1002/path.5248

Trivedi MK, Panda P, Sethi KK, Gangwar M, Mondal SC, Jana S (2020) Solid and liquid state characterization of tetrahydrocurcumin using XRPD, FT-IR, DSC, TGA, LC-MS, GC-MS, and NMR and its biological activities. J Pharm Anal 10(4): 334–345. https://doi.org/10.1016/j.jpha.2020.02.005

Umar A, Dunn BK, Greenwald P (2012) Future directions in cancer prevention. Nat Rev Cancer 12: 835–848. https://doi.org/10.1038/nrc3397

Venkatachalam K, Vinayagam R, Arokia Vijaya Anand M, Isa NM, Ponnaiyan R (2020) Biochemical and molecular aspects of 1,2-dimethylhydrazine (DMH)-induced colon carcinogenesis: a review. Toxicol Res (Camb) 9(1): 2-18. https://doi.org/10.1093/toxres/tfaa004

Weis SM, Cheresh DA (2011) Tumor angiogenesis: molecular pathways and therapeutic targets. Nat Med 17(11): 1359–1370. https://doi.org/10.1038/nm.2537

Yodkeeree S, Garbisa S, Limtrakul P (2008) Tetrahydrocurcumin inhibits HT1080 cell migration and invasion via downregulation of MMPs and uPA. Acta Pharmacol Sin 29: 853–860. https://doi.org/10.1111/j.1745-7254.2008.00792.x

Yoysungnoen P, Wirachwong P, Changtam C, Suksamrarn A, Patumraj S (2008) Anti-cancer and anti-angiogenic effects of curcumin and tetrahydrocurcumin on implanted hepatocellular carcinoma in nude mice. World J Gastroenterol 14(13): 2003-2009. https://doi.org/10.3748/wjg.14.2003

Yoysungnoen B, Bhattarakosol O, Changtam C, Patumraj S (2016) Combinational treatment effect of tetrahydrocurcumin and

celecoxib on cervical cancer cell-induced tumor growth and tumor angiogenesis in nude mice. J Med Assoc Thai 99(suppl. 4): S23-S31.

Yuan Z, Sheng D, Jiang L, Shafiq M, Khan AUR, Hashim R, Chen Y, Li B, Xie X, Chen J, Morsi Y, Mo X, Chen S (2022) Vascular endothelial growth factor-capturing aligned electrospun polycaprolactone/gelatin nanofibers promote patellar ligament regeneration. Acta Biomater 140: 233–246. https://doi.org/10.1016/j.actbio.2021.11.040

Yu M, Wang H, Ding A, Golenbock DT, Latz E, Czura CJ, Fenton MJ, Tracey KJ, Yang H (2006) HMGB1 signals through toll-like receptor (TLR) 4 and TLR2. Shock 26(2): 174–179. https://doi.org/10.1097/01.shk.0000225404.51320.82

Zafar A, Alruwaili NZ, Imam SS, Alsaidan OA, Alharbi KS, Mostafa EM, Musa A, Gilani SJ, Ghoneim MM, Alshehri S, Sultana S, Mohan S (2022) Formulation of ternary genistein β-cyclodextrin inclusion complex: in vitro characterization and cytotoxicity assessment using breast cancer cell line. J. Drug Deliv Sci Technol 67: 102932. https://doi.org/10.1016/j.jddst.2021.102932

Zeng A, Yu X, Chen B, Hao L, Chen P, Chen X, Tian Y, Zeng J, Hua H, Dai Y, Zhao J (2023) Tetrahydrocurcumin regulates the tumor immune microenvironment to inhibit breast cancer proliferation and metastasis via the CYP1A1/NF-kappaB signaling pathway. Cancer Cell Int 23(1): 12. https://doi.org/10.1186/s12935-023-02850-9

AUTHOR CONTRIBUTION:

Contribution	Dewi FRP	Elfianah V	Mahira AH	Aulia HS	Putra JE	Tan SC	Lim V	Pramudya M	Wahyuningsih SPA
Concepts or ideas	x						x		
Design	x					x			x
Definition of intellectual content	x								
Literature search	x	x	x	x	x				
Experimental studies		x	x	x	x				
Data acquisition	x	x	x	x	x				
Data analysis	x							x	
Statistical analysis	x							x	
Manuscript preparation	x	x	x	x	x	x	x		
Manuscript editing	x	x	x	x	x	x	x	x	x
Manuscript review	x	x	x	x	x	x	x	x	x

Citation Format: Dewi FRP, Elfianah V, Mahira AH,Aulia HS, Putra JE, Tan SC, Lim V, Pramudya M, Wahyuningsih SPA (2025) Improving the anticancer efficacy of tetrahydrocurcumin via β-cyclodextrin inclusion complexation. J Pharm Pharmacogn Res 13(3): 968–978. https://doi.org/10.56499/jppres24.2153_13.3.968

Publisher's Note: All claims expressed in this article are solely those of the authors and do not necessarily represent those of their affiliated organizations, or those of the publisher, the editors and the reviewers. Any product that may be evaluated in this article, or claim that may be made by its manufacturer, is not guaranteed or endorsed by the publisher.

Open Access: This article is distributed under the terms of the Creative Commons Attribution 4.0 International License (http://creativecommons.org/ licenses/by/4.0/), which permits use, duplication, adaptation, distribution and reproduction in any medium or format, as long as you give appropriate credit to the original author(s) and the source, provide a link to the Creative Commons license and indicate if changes were made.